Available online at www.sciencedirect.com
ScienceDirect
Journal of Power Sources 175 (2008) 338–344
JOURNAL OF POWER SOURCES
www.elsevier.com/locate/jpowsour

A comparison of the artificial neural network model and the theoretical model used for expressing the kinetics of electrophoretic deposition of YSZ on LSM

Sian-Jie Ciou [a], Kuan-Zong Fung [a], Kai-Wei Chiang [b,*]

[a] *Department of Materials Science and Engineering, National Cheng Kung University, Tainan 70101, Taiwan*
[b] *Department of Geometrics, National Cheng Kung University, Tainan 70101, Taiwan*

Received 19 July 2007; received in revised form 9 September 2007; accepted 10 September 2007
Available online 15 September 2007

Abstract

In the present study, an artificial neural network (ANN) model and a theoretical model are established to predict the kinetic behavior of electrophoretic deposition (EPD). Both the theoretical model and the ANN model describe the kinetic behavior of EPD at a low-applied voltage (below 15 V) well. However, the theoretical model failed to predict the behavior at the higher applied voltages of 40 and 50 V. In contrast, the proposed ANN model not only showed enhanced numerical accuracy, but was also generic to other operational conditions as well. Compared to the theoretical model, the ANN model shows outstanding capability of predicting actual kinetic behavior.

Keywords: Electrophoretic deposition; Artificial neural network

1. Introduction

Various colloidal processes can form monolayer or multilayer ceramic materials. For example, slip casting [1] and tape-rolling [2] have been used for a long time. However, these processes are limited to relatively simple shapes. Recently, electrophoretic deposition (EPD) of ceramic powders has been successfully applied for various applications in the fields of superconducting coating production [3–6], the manufacture of phosphor screens [7,8], and fuel cell creation [9–12].

EPD is a two-step process: first, the charged colloidal particles in the suspension migrate to one of the electrodes under an external electric field. This migration step involves the bulk properties of the colloidal suspension, such as conductivity, viscosity, particle concentration and dispersion, surface-charge density as well as the local field strength in the bath [13,14]. Second, the deposition step involves a complex combination of electrochemical and aggregation phenomena. Producing dense and coherent deposit layers requires that the particles release their surface charge at the electrode [15]. Although several efforts have been made to investigate this process, there are still some unknowns about controlling the formation of EPD because many parameters, which have a highly non-linear relationship between them, need to be considered [16]. Therefore, some assumptions that simplify the numerical solution of the problem are considered necessary to construct a proper model. However, assumptions could lead to a bias when comparing the model with the real system, thus making practical application much more difficult.

Statistical design of experiments used for the optimization of linear and non-linear systems allows the effects of several different factors to be analyzed and combined into a response model [17]. There are difficulties in symbolic and heuristic knowledge processing when using traditional algorithmic programming methods. An empirical method, called artificial neural networks (ANNs), has been used extensively by experts from engineering and science. The ANN can learn the system performance characteristics from existing data and then generalize what it has learnt [18–20]. Optimizing the network parameters, such as weights, can enhance the training rate and accuracy. Since 1980, interest in neural network computing has grown rapidly. Neural networks have been widely used in the estimation of the power system [21–32]. ANN is considered one of the best approaches to non-linear calibration and fitting problem in every field of chemistry.

* Corresponding author. Tel.: +886 6 2757575x63829.
E-mail address: kwchiang@mail.ncku.edu.tw (K.-W. Chiang).

0378-7753/$ – see front matter © 2007 Elsevier B.V. All rights reserved.
doi:10.1016/j.jpowsour.2007.09.024

Nomenclature

b_k	external bias
C	the particle concentration in suspension
d_{dep}	the thickness of the deposit
E	the error function
f	Hamaker factor
L	the distance from cathode to anode
M	the number of output neurons
n_h	the number of hidden neurons
n_χ	the number of external inputs
N	the pattern number in the training data
q	the slop parameter
$r_{deposited}$	resistivity of the deposited layer
$r_{suspension}$	resistivity of the suspension
V_{app}	the applied electric voltage
V_{real}	the actual voltage that affects the motion of particles
w	the deposited weight on the working electrode
w_{ij}, W_{ij}	the weight links
y_j^h	output from jth hidden neuron
y_{pq}	the desired output value of neuron q in the output layer for the training data
$\hat{y}_{pq}$	the real output value of neuron q in the output layer for the training data

Greek symbols

α	the learning rate
β	the constant that is added to the weight correction to stabilize vibration in the weights
χ	external inputs
ε_0	the permittivity of a vacuum
ε_r	the relative permittivity of the solvent
η	the viscosity of the solvent
μ	the electrophoretic mobility
θ	parameter vector
ζ	the zeta potential of suspension particles
Φ, af, AF	activation function

In this study, statistical experimental modeling using ANNs for yttria-stabilized zirconia (YSZ) deposition on $La_{0.85}Sr_{0.15}MnO_3$ (LSM) substrates is discussed and then compared with the theoretical model proposed by others [33]. The proposed architecture of ANNs is composed of a multilayer feed-forward neural network with a single hidden layer and trained with the back-propagation algorithm modified by a genetic algorithm (GA).

2. Theoretical background

2.1. The factors effecting EPD

The mechanisms of EPD include charged colloidal particles in solution moving under an applied external voltage, depositing particles onto an electrode where electrochemical reaction, i.e. charge transfer, takes place. Two groups of parameters determine the characteristics of this process: (a) the specific characteristics of the suspensions and (b) the physico-chemical parameters of the electrochemical cells, such as the conductivity of electrodes and the applied voltage.

For the EPD of particles, part of the current is carried by either the charged particles or free ions in the solution. So the amount of deposited particles does not depend only on the current, and it is believed that the ions accumulated at the electrodes restrict subsequent deposition [34]. However, the number of free ions is generally small in organic suspensions, such as ethanol. Therefore, the influence of accumulated ions is negligible.

The first attempt to correlate the number of particles with the parameters in EPD was proposed by Hamaker [13,14] and Augustinik et al. [35]. Hamakers law takes the following form:

$$w = f \int_{t_2}^{t_1} \mu \frac{V_{app}}{L} AC \, dt \tag{1}$$

It relates the deposited weight (w) to the applied electric voltage (V_{app}), the electrophoretic mobility (μ), the distance from cathode to anode (L), and the particle concentration in suspension (C). The Hamaker factor (f) is obtained by fitting experimental data, and its value is between 0 and 1. In the present study, the value of f is about 0.45 with a deviation of about 0.03.

Ishihara et al. [12], and Chen and Liu [33] used the expression by assuming that all particles in suspension are spherical and that the mobility of particles could be approximated by Henry's equation [36]:

$$w = f \frac{2}{3} C \varepsilon_0 \varepsilon_r \zeta \left(\frac{1}{\eta}\right) \left(\frac{V_{app}}{L}\right) t \tag{2}$$

where ε_0 is the permittivity of a vacuum, ε_r the relative permittivity of the solvent, ζ the zeta potential of suspension particles, and η is the viscosity of the solvent.

The applied electric field, V_{app}, which affects the motion of colloidal particles in suspension, decreases with increasing thickness of the deposited layer. Therefore, the voltage must be modified as [37]:

$$V_{real} = V_{app} \left(1 - \frac{d_{dep}}{d_{dep} + (L - d_{dep}) r_{suspension}/r_{deposited}}\right) \tag{3}$$

where V_{real} is the actual voltage that affects the motion of particles, d_{dep} the thickness of the deposit, and $r_{suspension}$ and $r_{deposited}$ are the resistivity of the suspension and the deposited layer, respectively. Therefore, the modified equation takes the form:

$$w = \frac{2}{3} f C \varepsilon_0 \varepsilon_r \zeta \left(\frac{1}{\eta}\right) \left(\frac{V_{real}}{L}\right) t = \frac{2}{3} f C \varepsilon_0 \varepsilon_r \zeta \left(\frac{t}{\eta}\right) \left(\frac{V_{app}}{L}\right) \times \left(1 - \frac{d_{dep}}{d_{dep} + (L - d_{dep}) r_{suspension}/r_{deposited}}\right) \tag{4}$$

2.2. Introductions to ANNs

ANNs are computer programs based on a simplified model of the brain and can be applied to map the relationships of multivariate data. There are several types of neural network

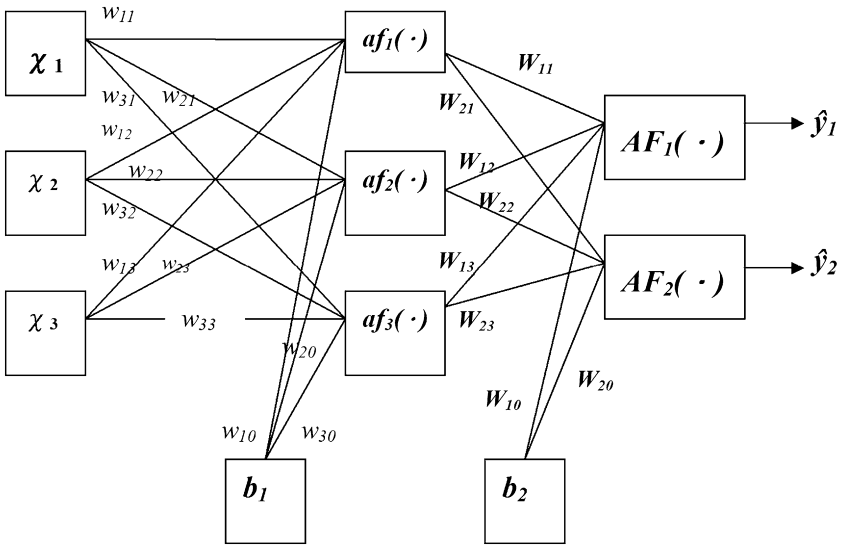

Fig. 1. A schematic of the architecture of an ANN.

architectures, but the most common one is the multilayer feed-forward neural network. Generally speaking, the structure of a multilayer feed-forward neural network is constructed from small processing units (neurons) that are interconnected within the network using weighted links. In general, the basic model of the neuron contains three major components: (a) weight links $\langle w_{j,l}, W_{i,j}\rangle$; (b) an adder (additive function) for summing the input signals χ_i that are weighted by respective synapses of the neuron and external bias (b_k); and (c) an activation function $\varphi(\cdot)$ for limiting the amplitude of the neuron output and the final output y_k. Fig. 1 depicts a feed-forward network which contains external inputs (χ_1, χ_2, χ_3), a hidden layer with two hidden neurons, and an output layer with two output neurons. The depicted network is said to be fully connected since all inputs/neurons in one layer are connected to all neurons in the following layer.

The mathematical formula expressing what is happening in the network takes the form:

$$\hat{y}_i(t) = \hat{f}(\chi, \theta) = \mathrm{AF}_i\left[\sum_{j=1}^{n_\mathrm{h}} W_{i,j}\,\mathrm{af}_j\left(\sum_{l=1}^{n_\phi} w_{j,l}\chi_l + w_{j,0}\right) + W_{i,0}\right] \quad (5)$$

θ specifies the parameter vector, which contains all the adjustable parameters of the network; i.e., the weights and biases $\langle w_{j,l}, W_{i,j}\rangle$. Since the bias can be interpreted as a weight acting on an input clamped to 1; i.e., b_1, $b_2 = 1$, the joint description "weight" covers both weights and bias. To determine the weight values, one must have a set of examples of how the outputs, $\hat{y}_i$, should relate to the inputs χ_l. The process of obtaining the weights from these examples is called supervised learning and is basically a conventional estimation process. That is, the weights are estimated from existing examples in such a way that the network, according to some metric, models the true relationship as accurately as possible. In Fig. 1, af(·) and AF(·) represent the activation functions for hidden neurons and output neurons. In this study, a non-linear activation function is utilized at the hidden neurons so that the non-linearities can enhance the network's approximation capabilities and reduce the impact of noise. A linear activation function is applied at the output layer neurons. Such combinations, one non-linear hidden layer and a linear output layer, have shown the ability to approximate any differentiable function [38]. The sigmoid activation function, which was used in the hidden layer, takes the form:

$$y_j^\mathrm{h} = \frac{1}{1+\exp\left[-q\left(\sum_{l=1}^{n_\phi} w_{j,l}\chi_l + w_{j,0}\right)\right]}, \quad j = 1, n_\mathrm{h} \quad (6)$$

where y_j^h represents the output of the jth hidden neuron, q the slop parameter, n_ϕ the number of external inputs, and n_h represents the number of hidden neurons. The linear activation function used in the output layer was the linear sigmoid function, which substitutes the intermediate portion of the sigmoid by a line, making it a piecewise linear approximation of the sigmoid:

$$y_j^\mathrm{h} = \begin{cases} 0, & -q\left(\sum_{l=1}^{n_\phi} w_{j,l}\chi_l + w_{j,0}\right) < 0 \\ 1, & -q\left(\sum_{l=1}^{n_\phi} w_{j,l}\chi_l + w_{j,0}\right) > 1 \quad (j = 1, n_\mathrm{h}) \\ -q\left(\sum_{l=1}^{n_\phi} w_{j,l}\chi_l + w_{j,0}\right), & \text{else} \end{cases} \quad (7)$$

A detailed description of ANNs can be found in Ref. [20].

Many learning algorithms can be used for training ANNs. The most frequently used algorithm is called back-propagation. The solution of the weights in feed-forward neural networks is a multivariate optimization problem where the connective weights are the variables to be optimized with cost functions equal to the sum of squared residual errors. In general, the error function (E) takes the form:

$$E = \frac{1}{2}\sum_{p=1}^{N} E_k = \frac{1}{2}\sum_{p=1}^{N}\sum_{q=1}^{M}(y_{pq} - \hat{y}_{pq}) \quad (8)$$

where y_{pq} is the desired output value of neuron q in the output layer for the training data and $\hat{y}_{pq}$ the real output, N the pattern number in the training data and M is the number of output neurons. The weights are modified by the following expression:

$$w_{ij}(k+1) = w_{ij} + \alpha\left(\frac{\partial E}{\partial w_{ij}}\right)_{w=w(jk)} + \beta[(w_{ij}(k) - w_{ij}(k-1)] \quad (9)$$

where α is the learning rate and β is a constant that is added to the weight correction to stabilize the vibration in the weights that occurs in the learning process. A more detailed discussion of the theory can be found in Ref. [39].

Some studies have combined both ANN and GA to model pharmaceutical processes [40]. Because ANNs consist of several variables, such as the number of layers, the number of neurons in each layer, and the values of weights, GA can be applied to optimize the calculation process of ANNs and to avoid the local minimum.

GA is used to search the solution space through the simulated evolution of generations of the fittest. These are used to solve linear and non-linear problems by exploring all regions of the state space and developing obscured areas through mutation, crossover, and selection operations applied to individuals in the population [41–43]. The procedure of GA includes: chromosome representation, a selection function, a mutation and crossover for the reproduction function, the formation of the initial population, termination criteria, and the evaluation function, as depicted in Fig. 2.

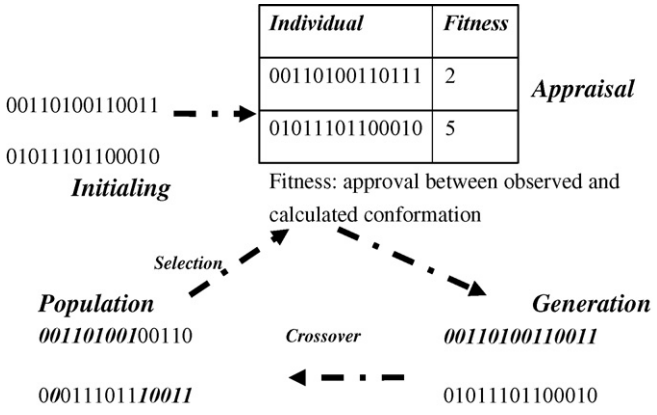

Fig. 2. Schematic representation of GA optimization.

3. Experimental procedure

3.1. Preparation of the LSM substrate

LSM powders were prepared by the precursors La_2O_3 (Alfa), MnO_2 (Aldrich), and $Sr(NO_3)_2$ (Aldrich). The stoichiometerical amounts of those precursors were mixed with ethanol (99.8% reagent grade, Kanto Chemicals, Tokyo, Japan). Afterward, the powders were milled, sieved, and calcined at 800 °C. Then, the calcined powders were pressed into the shape of a disk, and sintered at 1400 °C. The diameter of the LSM-disk after heat treatment was about 10 mm.

3.2. YSZ suspension for EPD

Suspensions with 0.1 vol% fraction of solid loads were consisted of ethanol (99.8% reagent grade, Kanto Chemicals, Tokyo, Japan) and the YSZ powder (TZ-8Y, Tosho). The YSZ powder must be washed in EtOH and H_2O by centrifuging before preparing the suspension until the conductivity of the solution was close to zero. The powder was dispersed in suspension using an ultrasonic horn (DC400H, Delta) for 30 min, and the pH was adjusted to 4.03 using acetic acid (Fluka).

3.3. EPD YSZ on the LSM substrate

For the EPD process, a carbon electrode was used as the anode and the prepared LSM-disk as the cathode, which was connected to a balance (Mettler 6900). The electrodes were set parallel to each other with a separation distance of 3 cm, and immersed into the YSZ suspension, which was kept at a constant temperature of 25 °C. A pH meter (TDK-5721S) was used to measure the pH variation during the entire process. The YSZ coatings were deposited at constant voltages of 10, 12.5, 15, 40, and 50 V, respectively. The deposition time was from 3 to 10 min.

3.4. Creation of the ANN model

A multilayer feed-forward neural network with a single hidden layer, as shown in Fig. 3, is proposed. The input parameters are the current density of the cathode, working temperature, pH, applied voltage, and deposition time. These inputs are passed forward to produce the outputs, which are the weight densities of deposited YSZ on the LSM electrode (per square centimeter). To optimize the network, a back-propagation algorithm modified by GA was used to train the ANNs.

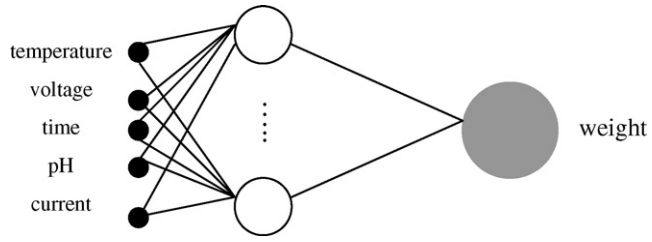

Fig. 3. ANN for the performance map of EPD.

3.5. Data pre-processing for training

The training examples have to be uniformly distributed throughout the operation range to achieve reasonable training as well as acceptable prediction accuracy; therefore, the training patterns must be selected carefully. Because of variation in the scale of inputs, the inputs were normalized from 0 to 1 to allow an efficient and correct training procedure. Generally speaking, pre-processed data improves the homogeneity of the parameters, which avoids neglecting values, which may be decisive to the overall performance of the proposed scheme.

3.6. The training process

The experimental data for training the ANNs was inputted repeatedly until the desired goal was reached. When the network finishes learning, the training error will converge to zero. However, smaller training error does not necessarily imply a better network prediction accuracy when new input data is applied. If the training error threshold is set to be too small, it is possible to over-train a network. As a result, the prediction accuracy of new and omitted inputs deteriorates. To avoid this predicament, cross-validation, which is a popular criterion to prevent over-training, was used in this study [44]. As a result, 50 sets of data were picked from each recorded experimental result, representing EPD at 10, 12.5, 15, 40, and 50 V, respectively, as testing data. The remaining sets were separated into 90% and 10% as the training and cross-validation data, respectively. Because there was no prior information about a suitable ANN structure for predicting the EPD process, an ANN model with one hidden layer with 25 neurons was used in the present study, and the values of weights were initially random. Traditionally, the number of neurons in the hidden layer is decided by trial-and-error. However, GA can help an ANN model to decide the number of neurons in the hidden layer. Other than the number of neurons in the hidden layer, the adjustable parameters of the ANN model, such as weights, training epochs, and learning rates, were also modified automatically by GA, with the training process continuing until the desired accuracy was reached. The lowest mean square error (MSE) was selected as the training endpoint for all networks. After the proper ANN model was built, the experimental data was combined with former data and processed in the model to make the ANN model learn new information.

4. Results and discussion

The parameters in the theoretical model based on Eq. (4) are listed in Table 1, and the voltage drops of each applied voltage are given in Fig. 4. These voltages drops were calculated based on Eq. (3), and the thickness variation of deposited layers was measured at regular intervals.

Figs. 5–9 show the deposited YSZ weight using EPD at 10, 12.5, 15, 40, and 50 V, respectively. The solid line represents the experimental data; the theoretical predictions based on Eq. (4) are represented by squares dots; the diamonds represent the ANN predictions. In Figs. 5–7, it can be seen that both the theoretical model and the ANN model predicted the YSZ deposition

Table 1
Parameter values in the theoretical model based on Eq. (4)

Description	Notation	Unit	Value
Initial concentration of YSZ	C^*_{YSZ}	$g\,l^{-1}$	3.96×10^{-9}
Viscosity of ethanol	η	Pa s	1.074×10^{-3}
Distance between the cathode and anode	L	m	3×10^{-2}
Zeta potential of YSZ	ζ_p	mV	40.3
The actual voltage that affects the motion of colloidal particles	V_{app}	V	10, 12.5, 15 40, 50
Dielectric constant of vacuum	ε_0	$C^2\,N^{-1}\,m^{-2}$	8.854×10^{-12}
Relative dielectric constant of the pure ethanol	ε_r	NaN	24.3

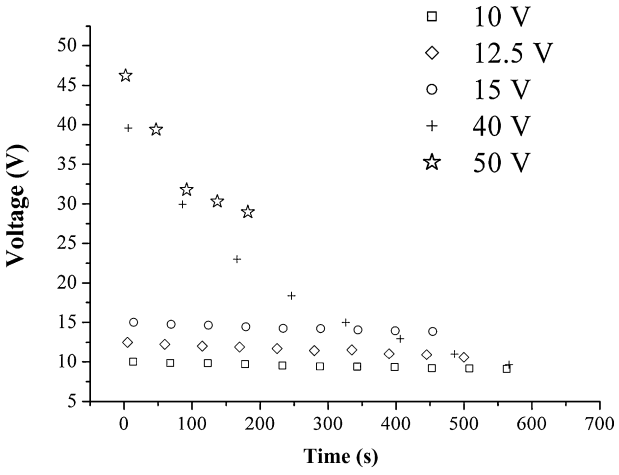

Fig. 4. The voltage variation during EPD at different applied voltages.

weight accurately. The standard deviation, which indicates the difference between experimental data and the predictions, was 0.00030 and 0.00035 for the ANN model and the theoretical model, respectively. There was no doubt that both models were able to describe the behavior of EPD at a low-applied voltage (10, 12.5 and 15 V). However, the standard deviation for the theoretical model increased with increasing applied voltage; the

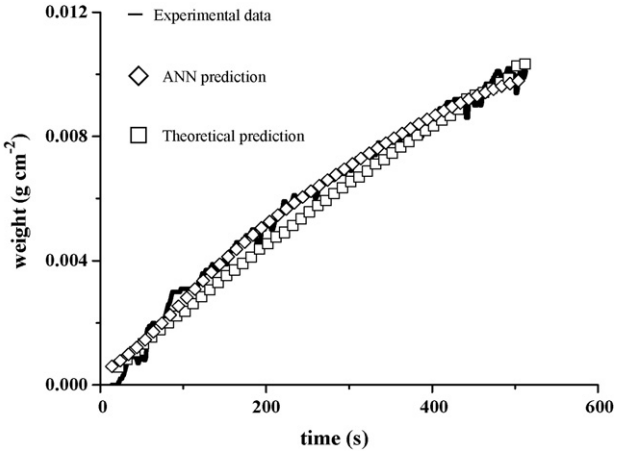

Fig. 5. The experimental data (—); the ANN prediction (◊); and the theoretical prediction (□) for EPD at 10 V.

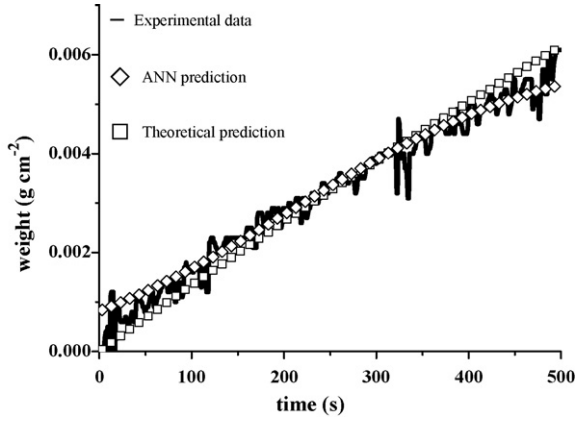

Fig. 6. The experimental data (—); the ANN prediction (◊); and the theoretical prediction (□) for EPD at 12.5 V.

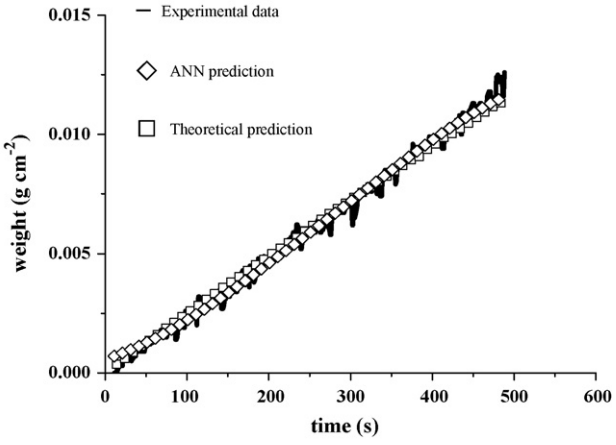

Fig. 7. The experimental data (—); the ANN prediction (◊); and the theoretical prediction (□) for EPD at 15 V.

standard deviation was 0.00503 for 40 V and 0.0170 for 50 V. For the ANN model, the standard deviation increased to 0.00196 for 40 V and 0.00673 for 50 V. The standard deviations are listed in Table 2. Although the accuracy of both the theoretical model and ANN model decreased with increasing applied voltage, the

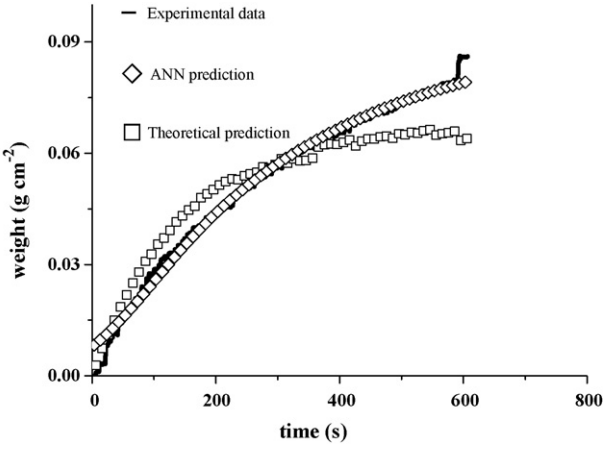

Fig. 8. The experimental data (—); the ANN prediction (◊); and the theoretical prediction (□) for EPD at 40 V.

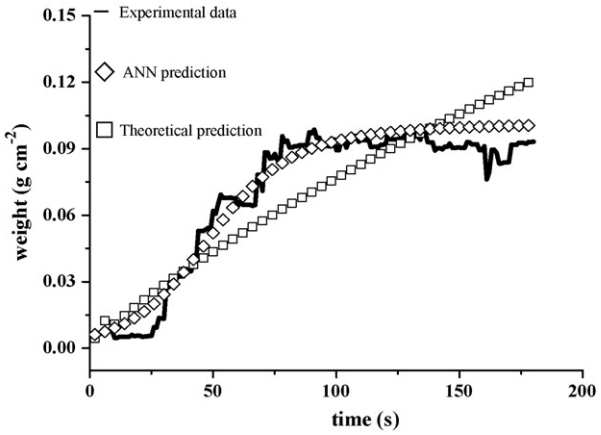

Fig. 9. The experimental data (—); the ANN prediction (◊); and the theoretical prediction (□) for EPD at 50 V.

Table 2
The standard deviation (the difference between experimental data and prediction) of the theoretical and the ANN models

Standard deviation	Theoretical prediction (□)	ANN model (◊)
10 V	0.00035	0.00025
12.5 V	0.00034	0.00028
15 V	0.00036	0.00030
40 V	0.00503	0.00196
50 V	0.01701	0.00673

ANN model was much better at higher applied voltages (40 and 50 V). In Figs. 8 and 9, the exponential-decay tendency of EPD, which is different from the linear relationship in Figs. 5–7, can be observed. The ANN model showed a much better fit than did the theoretical model to the behavior of EPD. The ANN model is accurate and flexible.

5. Conclusion

In the present study, the proposed ANN model and a theoretical model were established to predict the kinetic behavior of EPD. Both demonstrated the ability to predict the amount of deposited weight of YSZ accurately at applied voltages below 15 V. However, some unknowns, such as the Hamaker constant *f*, in the theoretical model, make it complicated to optimize the process quantitatively and apply it practically. Furthermore, the deviation at higher applied voltages, beyond 40 V, was too high to describe the behavior of EPD precisely.

The ANN model is a powerful tool for solving system identification problems. Besides enhancing accuracy, the ANN model showed the ability to be much more flexible in every operational condition and easier to use in this research; therefore, it is suitable for the generation of performance maps.

References

[1] J. Requena, R. Moreno, J.S. Moya, J. Am. Ceram. Soc. 72 (1989) 1511–1513.
[2] W.J. Clegg, Acta Metall. Mater. 40 (1992) 3085–3093.
[3] H.S. Maiti, S. Datta, R.N. Basu, J. Am. Ceram. Soc. 72 (1989) 1733–1735.

[4] C.T. Chu, B. Dunn, Appl. Phys. Lett. 55 (1989) 492–494.
[5] H. Nojima, H. Shintaku, M. Nagaa, M. Koda, Jpn. J. Appl. Phys. 30 (1991) 1166–1168.
[6] M. Nagai, K. Yamashita, T. Umegaki, Y. Takuma, J. Am. Ceram. Soc. 76 (1993) 253–255.
[7] J.A. Siracuse, J.B. Talbot, E. Sluky, T. Avalos, K.R. Hesse, J. Electrochem. Soc. 137 (1990) 2336–2340.
[8] M.J. Shane, J.B. Talbot, B.G. Kinney, E. Sluzky, K.R. Hesse, J. Colloid Interf. Sci. 165 (1994) 334–340.
[9] R.W. Powers, Am. Ceram. Soc. Bull. 65 (1986) 1270–1277.
[10] R.W. Powers, Am. Ceram. Soc. Bull. 65 (1986) 1277–1281.
[11] H. Negishi, K. Yamaji, T. Imura, D. Kitamoto, T. Ikegami, H. Yanagishita, J. Electrochem. Soc. 152 (2005) J16–J22.
[12] T. Ishihara, K. Shimose, T. Kudo, H. Nishiguchi, T. Akbay, Y. Takita, J. Am. Ceram. Soc. 83 (2000) 1921–1927.
[13] H.C. Hamaker, Trans. Faraday Soc. 35 (1940) 186–191.
[14] H.C. Hamaker, E.J.W. Verwey, Trans. Faraday Soc. 35 (1940) 180–185.
[15] E. de Beer, J. Duval, E.A. Meulenkamp, J. Colloid Interf. Sci. 222 (2000) 117–124.
[16] G. Anné, K. Vanmeensel, J. Vleugels, O. van der Biest, J. Am. Ceram. Soc. 88 (2005) 2036–2039.
[17] D.C. Montgomery, Design and Analysis of Experiments, 5th ed., John Wiley & Sons, New York, 2001, pp. 101–110.
[18] J. Gasteiger, J. Zupan, Angew. Chem. Int. Ed. Engl. 32 (1993) 503–527.
[19] S.N. Jordan, A.R. Leach, J. Bradshaw, J. Chem. Inf. Comput. Sci. 35 (1995) 640–650.
[20] M.T. Hagan, H.B. Demuth, M. Beale, Neural Network Design, PWS, 1996, pp. 324–330.
[21] R. Sousa, F. Colmati, E.R. Gonzalez, J. Power Sources 161 (2006) 183–190.
[22] C. Nitsche, S. Schroedl, W. Weiss, E. Pucher, J. Power Sources 145 (2005) 383–391.
[23] H. Karami, M.F. Mousavi, M. Shamsipur, S. Riahi, J. Power Sources 154 (2006) 298–307.
[24] S.O.T. Ogaji, R. Singh, P. Pilidis, M. Diacakis, J. Power Sources 154 (2006) 192–197.
[25] R.E. Young, L. Xiang, S.P. Perone, J. Power Sources 62 (1996) 121–134 .
[26] J. Arriagada, P. Olausson, A. Selimovic, J. Power Sources 112 (2002) 54–60.
[27] S. Ou, E.K.L. Achenie, J. Power Sources 140 (2005) 319–330.
[28] C.C. Chan, E.W.C. Lo, S. Weixiang, J. Power Sources 87 (2000) 201–204.
[29] S. Jemeï, D. Hissel, M.C. Péra, J.M. Kauffmann, J. Power Sources 124 (2003) 479–486.
[30] E. Entchev, L. Yang, J. Power Sources 170 (2007) 122–129.
[31] H. Karami, M.A. Karimi, M. Mahdipour, J. Power Sources 158 (2006) 936–943.
[32] A. Urbina, T.L. Paez, R.G. Jungst, B.Y. Liaw, J. Power Sources 110 (2002) 430–436.
[33] F. Chen, M. Liu, J. Eur. Ceram. Soc. 21 (2001) 127–134.
[34] L. Besra, M. Liu, Mater. Sci. 52 (1) (2007) 1–61.
[35] A.I. Augustinik, V.S. Vigdergauz, G.I. Zharavlev, J. Appl. Chem. 35 (1962) 2175–2180.
[36] R.J. Hunter, Foundations of Colloid Science, 1, 1st ed., Clarendon Press, Oxford, UK, 1987, pp. 265–270.
[37] G. Anné, B. Neirinck, K. Vanmeensel, O. Van der Biest, J. Vleugels, J. Am. Ceram. Soc. 89 (2006) 823–828.
[38] R.D. Reed, R.J. Marks, Neural Smoothing Supervised Learning in Feedforward Artificial Neural Networks, The MIT press, 1999, pp. 187–191.
[39] D. Rumelhart, G. Hinton, R. Williams, Learning internal representations by error propagation, in: D. Rumelhart, J. McClelland (Eds.), Parallel Distributed Processing: Explorations in the Microstructure of Cognition, vol. 1, MIT Press, Cambridge, MA, 1986, pp. 318–362.
[40] S. Agatonovic-Kustrin, R.G. Alany, Pharm. Res. 18 (7) (2001) 110–115.
[41] J.H. Holland, Adoption in Natural and Artificial Systems, University of Michigan Press, Ann Arbor, Ml, 1975, pp. 95–102.
[42] D.E. Goldbergm, Gentic Algorithms in Search, Optimization, and Machine Learning, Addison–Wesley, Reading, MA, 1989, pp. 32–40.
[43] D.J. Montana, L. Davis, Proceedings of the 11th International Joint Conference on Artificial Intelligence, vol. 1, Morgan Kaufmann, San Mateo, CA, 1989, pp. 762–767.
[44] J.C. Principe, N.R. Euliano, W.C. Lefebvre, Neural and Adaptive Systems: Fundamentals Through Simulations, John Wiley & Sons, New York, 2000, pp. 15–21.